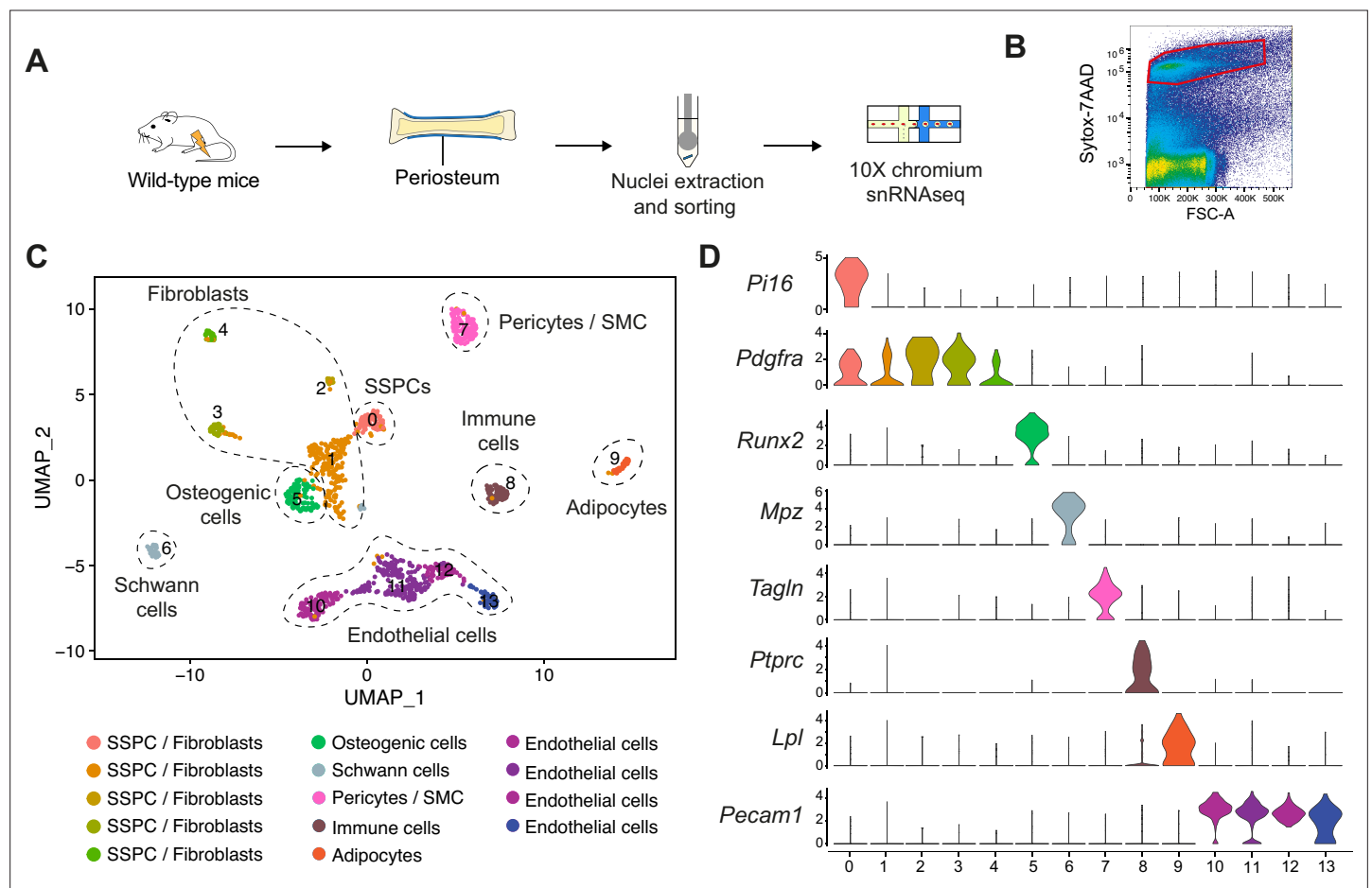


---

## Figures and figure supplements

Single-nucleus transcriptomics reveal the differentiation trajectories of periosteal skeletal/stem progenitor cells in bone regeneration

**Simon Perrin et al.**



**Figure 1.** Heterogeneity of the periosteum at steady state. **(A)** Experimental design. Nuclei were extracted from the periosteum of uninjured tibia and processed for single-nucleus RNAseq. **(B)** Sorting strategy of nuclei stained with Sytox-7AAD for snRNAseq. Sorted nuclei are delimited by a red box. **(C)** UMAP of color-coded clustering of the uninjured periosteum dataset. Eight populations are identified and delimited by black dashed lines. **(D)** Violin plots of key marker genes of the different cell populations.

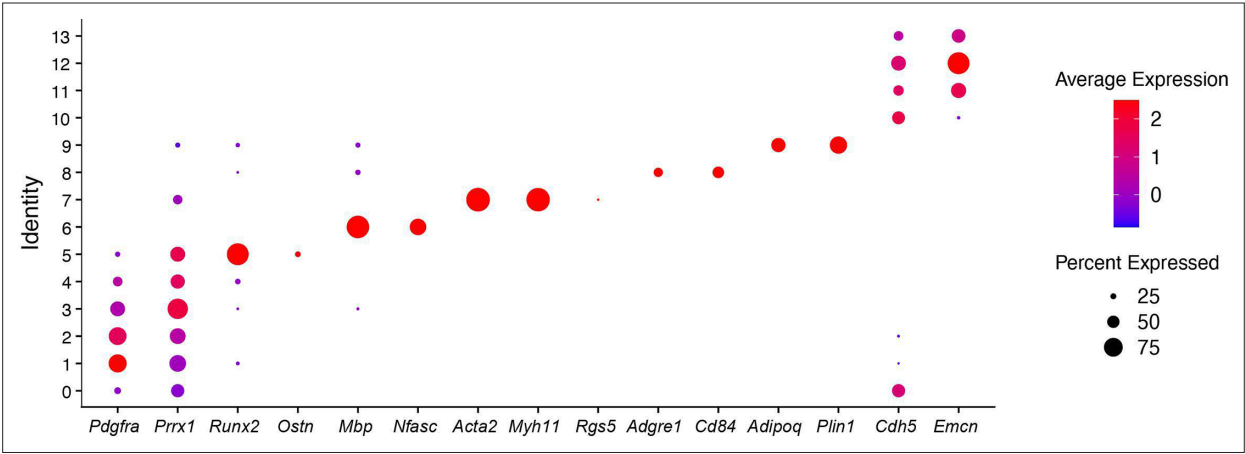


**Figure 1—figure supplement 1.** Dot plot of marker genes of the populations from uninjured periosteum.

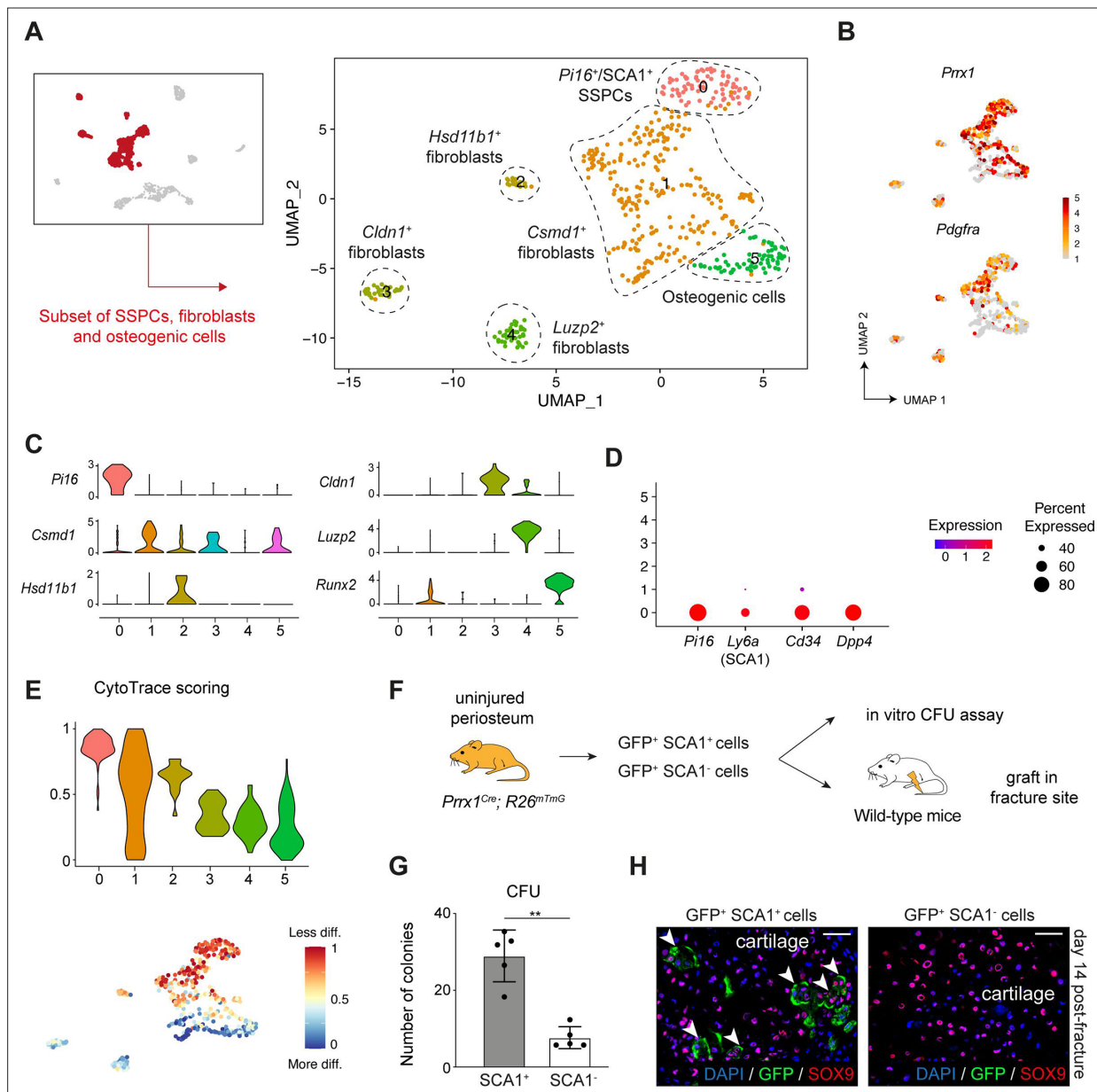


**Figure 2.** Identification of periosteal skeletal stem/progenitor cells in the intact periosteum. **(A)** UMAP of color-coded clustering of the subset of SSPCs/fibroblasts. **(B)** Feature plots of *Prx1* and *Pdgfra* in the subset of SSPCs/fibroblasts. **(C)** Feature plots of key marker genes of the different cell populations. **(D)** Dot plot of the stemness markers *Pi16*, *Ly6a* (SCA1), *Cd34*, and *Dpp4*. **(E)** Violin and feature plots of CytoTrace scoring in the subset of SSPCs/fibroblasts, showing that SCA1 expressing SSPCs (cluster 0) are the less differentiated cells in the dataset. **(F)** Experimental design: GFP<sup>+</sup> SCA1<sup>+</sup> and GFP<sup>+</sup> SCA1<sup>-</sup> were isolated from uninjured tibia of *Prx1*<sup>Cre</sup>; *R26*<sup>mTmG</sup> mice and used for in vitro CFU assays or grafted at the fracture site of wild-type mice. **(G)** In vitro CFU assay of murine periosteal *Prx1*-GFP<sup>+</sup> SCA1<sup>+</sup> and *Prx1*-GFP<sup>+</sup> SCA1<sup>-</sup> cells (n = 5 biological replicates from 2 distinct experiments). **(H)** High magnification of SOX9 immunofluorescence of callus section 14 days post-fracture showing that GFP<sup>+</sup> SCA1<sup>+</sup> cells contribute to the callus (white arrowheads) while GFP<sup>+</sup> SCA1<sup>-</sup> cells are not contributing (n = 3 per group).



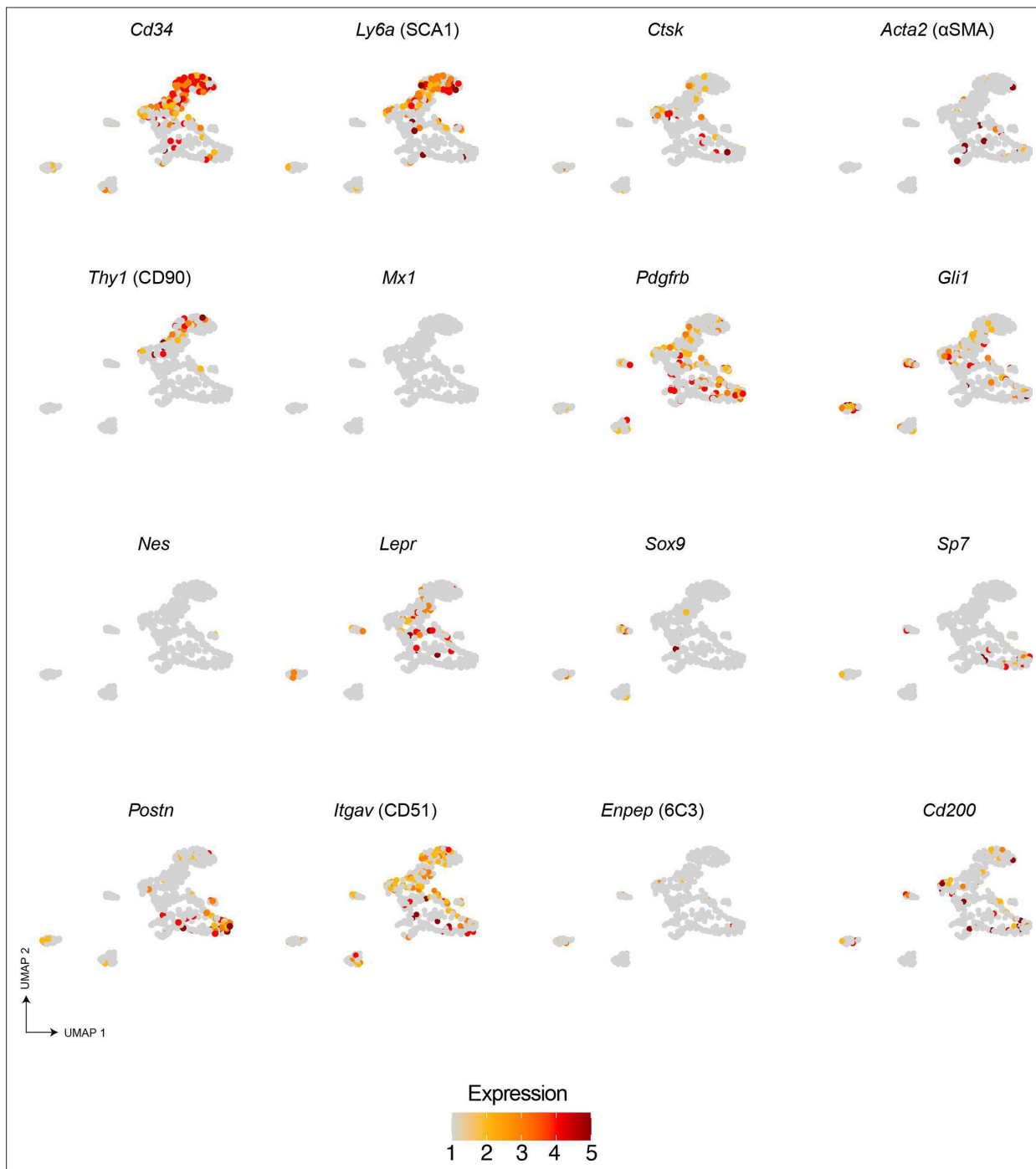


**Figure 2—figure supplement 1.** Expression of known skeletal stem/progenitor cell (SSPC) markers in the periosteum at steady state. Feature plots of known markers of SSPCs in the SSPC/fibroblast subset of the periosteum at steady state.

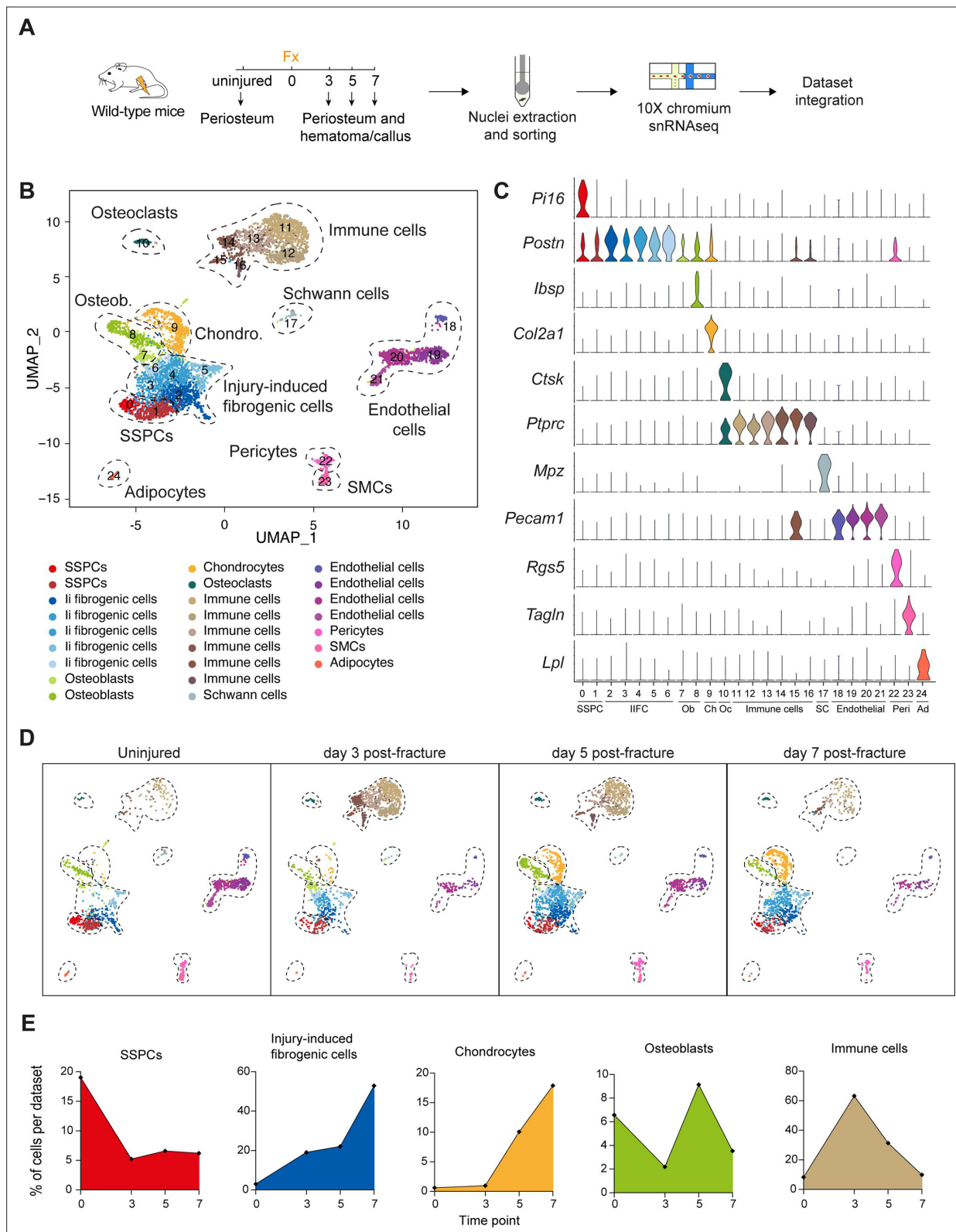
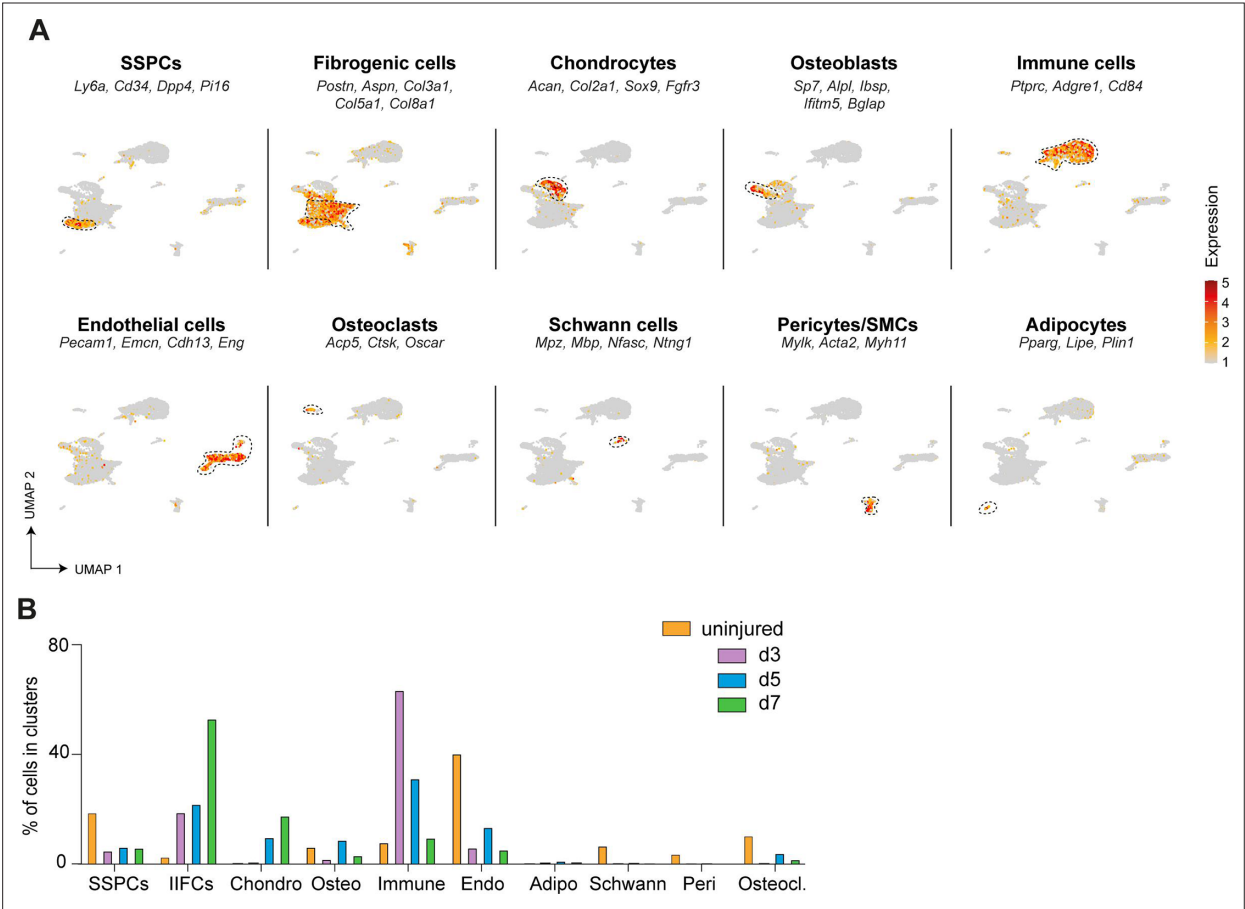


**Figure 3.** Periosteal response to fracture at single-nucleus resolution. **(A)** Experimental design. Nuclei were extracted from the periosteum of uninjured tibia and from the injured periosteum and hematoma/callus at days 3, 5, and 7 post-tibial fracture of wild-type mice and processed for single-nucleus RNAseq. **(B)** UMAP of color-coded clustering of the integration of uninjured, day 3, 5, and 7 datasets. Eleven populations are identified and delimited by black dashed lines. **(C)** Violin plots of key marker genes of the different cell populations. **(D)** UMAP of the combined dataset separated by time

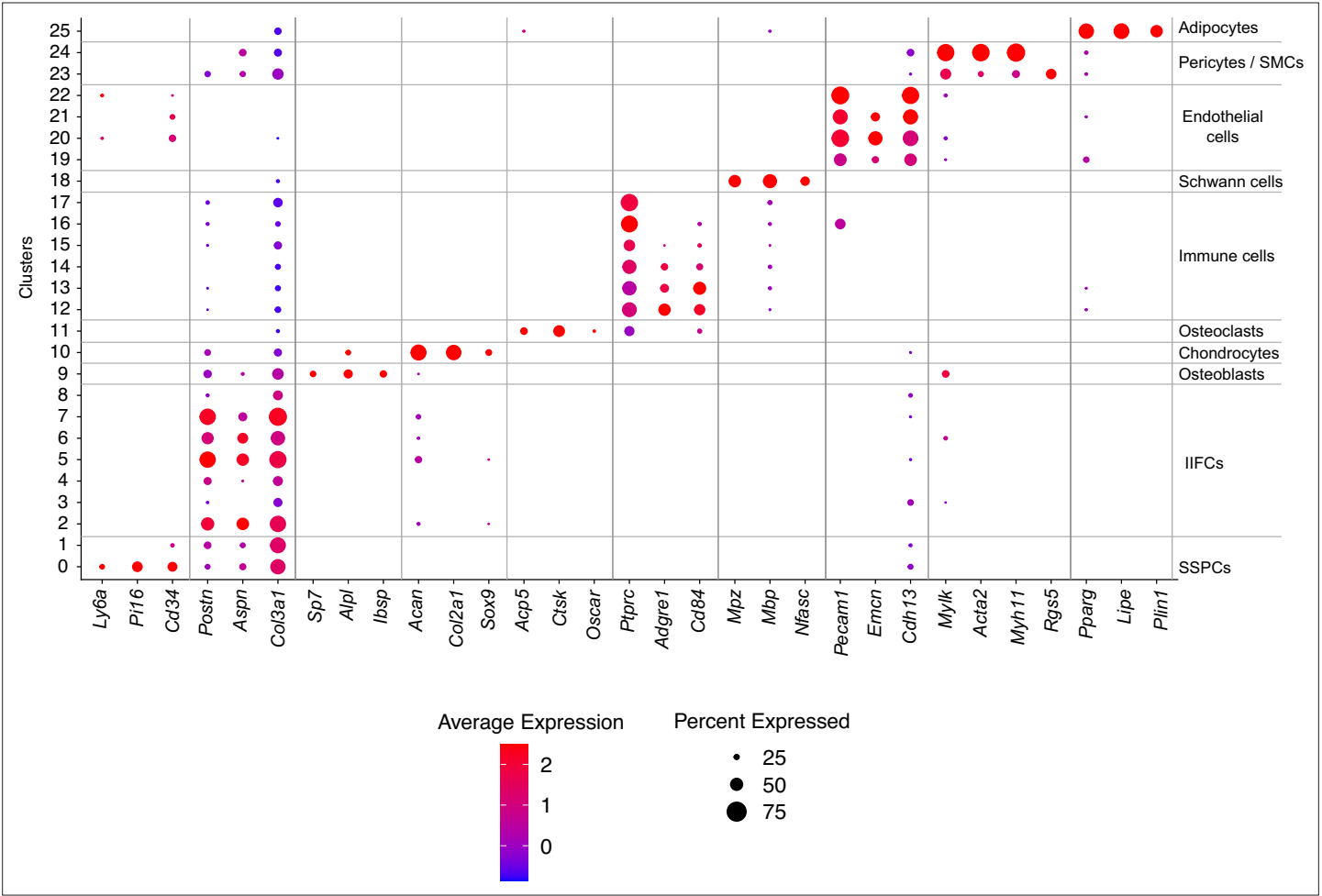
Figure 3 continued on next page

Figure 3 continued

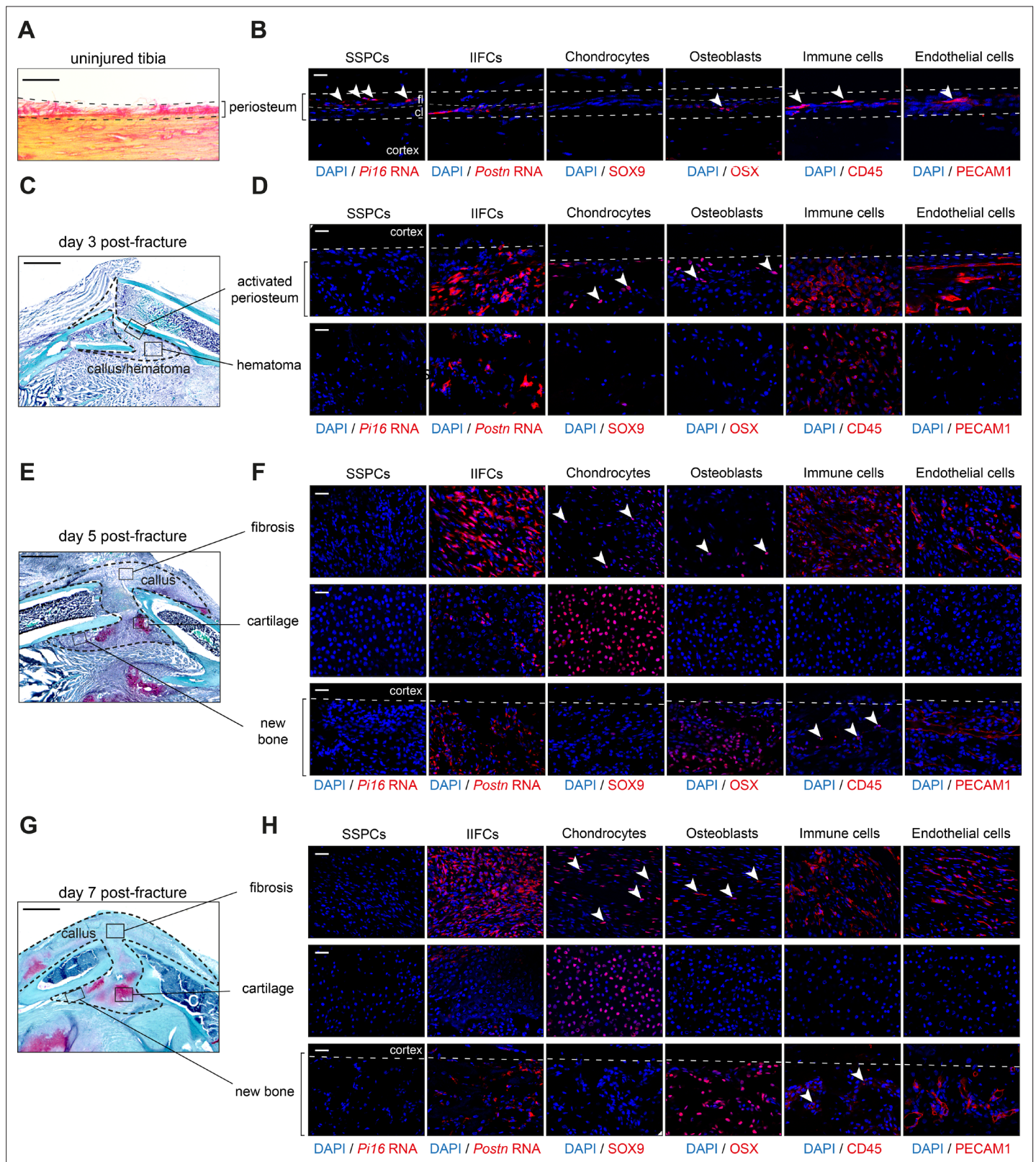
point. **(E)** Percentage of cells in skeletal stem/progenitor cell (SSPC), injury-induced fibrogenic cell, osteoblast, chondrocyte, and immune cell clusters in uninjured, day 3, 5, and 7 datasets.



**Figure 3—figure supplement 1.** Heterogeneity and dynamics of the cell populations in the fracture environment. **(A)** Feature plots of the lineage score of the different cell populations in the combined fracture datasets. **(B)** Percentage of cells in each cell population per time point.



**Figure 3—figure supplement 2.** Dot plot of marker genes of the populations from the combined fracture dataset.



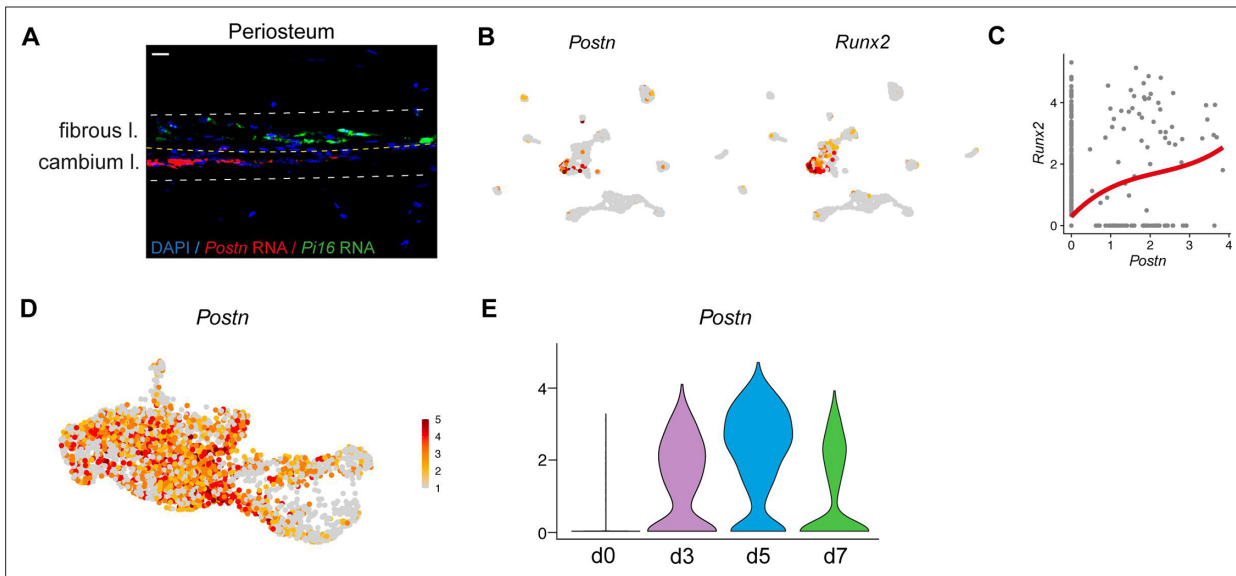
**Figure 4.** Cellular organization of the fracture callus. (A) Picrosirius staining of the uninjured periosteum. (B) Immunofluorescence and RNAscope on adjacent sections show the presence of SSPCs (*Pi16*-expressing cells) in the fibrous layer (fl), *Postn*-expressing cells in the cambium layer (cl), *OSX*<sup>+</sup> osteoblasts, immune cells (*CD45*<sup>+</sup>), and endothelial cells (*PECAM1*<sup>+</sup>) in the periosteum (n = 3 per group). (C) Safranin'O staining of longitudinal callus sections at day 3 post-tibial fracture. (D) Immunofluorescence and RNAscope on adjacent sections show absence of skeletal stem/progenitor

Figure 4 continued on next page

## Figure 4 continued

cells (SSPCs) (*Pi16*<sup>+</sup>), and presence of IIFCs (*Postn*<sup>+</sup>) and immune cells (CD45<sup>+</sup>) in the activated periosteum and hematoma at day 3 post-fracture. Chondrocytes (SOX9<sup>+</sup>, white arrowhead), osteoblasts (OSX<sup>+</sup>, white arrowhead), immune cells (CD45<sup>+</sup>), and endothelial cells (PECAM1<sup>+</sup>) are detected in the activated periosteum (n = 3 per group). **(E)** Safranin'O staining of longitudinal callus sections at day 5 post-tibial fracture. **(F)** Immunofluorescence and RNAscope on adjacent sections show injury-induced fibrogenic cells (IIFCs) (*Postn*<sup>+</sup>), chondrocytes (SOX9<sup>+</sup>, white arrowhead), osteoblasts (OSX<sup>+</sup>, white arrowhead), immune cells (CD45<sup>+</sup>), and endothelial cells (PECAM1<sup>+</sup>) in the fibrosis, chondrocytes (SOX9<sup>+</sup>) in the cartilage and osteoblasts (OSX<sup>+</sup>), immune cells (CD45<sup>+</sup>, white arrowhead), and endothelial cells (PECAM1<sup>+</sup>) in the new bone (n = 3 per group). **(G)** Safranin'O staining of longitudinal callus sections at day 7 post-tibial fracture. **(H)** Immunofluorescence and RNAscope on adjacent sections show IIFCs (*Postn*<sup>+</sup>), chondrocytes (SOX9<sup>+</sup>, white arrowhead), osteoblasts (OSX<sup>+</sup>, white arrowhead), immune cells (CD45<sup>+</sup>), and endothelial cells (PECAM1<sup>+</sup>) in the fibrosis, chondrocytes (SOX9<sup>+</sup>) in the cartilage and osteoblasts (OSX<sup>+</sup>), immune cells (CD45<sup>+</sup>, white arrowhead), and endothelial cells (PECAM1<sup>+</sup>) in the new bone (n = 3 per group). Scale bars: **(A–B–E)** 1 mm, **(B–D–F)** 100  $\mu$ m.





**Figure 4—figure supplement 1.** Periosteal skeletal stem/progenitor cells do not express *Postn*. **(A)** RNAscope experiment showing the presence of *Postn* expressing cells in the inner cambium layer (cambium I.) of the periosteum and *Pi16*-expressing cells in the fibrous layer (fibrous I.). **(B)** Feature plots of *Postn* and *Runx2* expression in the uninjured periosteum. **(C)** Scatter plot of *Runx2* and *Postn* expression in the uninjured periosteum dataset showing that *Postn* is mostly expressed by cells expressing *Runx2*. **(D)** Feature plot of *Postn* expression in the subset of SSPCs, injury-induced fibrogenic cells (IIFCs), osteogenic and chondrogenic cells from **Figure 5B**. **(E)** Violin plot of *Postn* expression per time point.



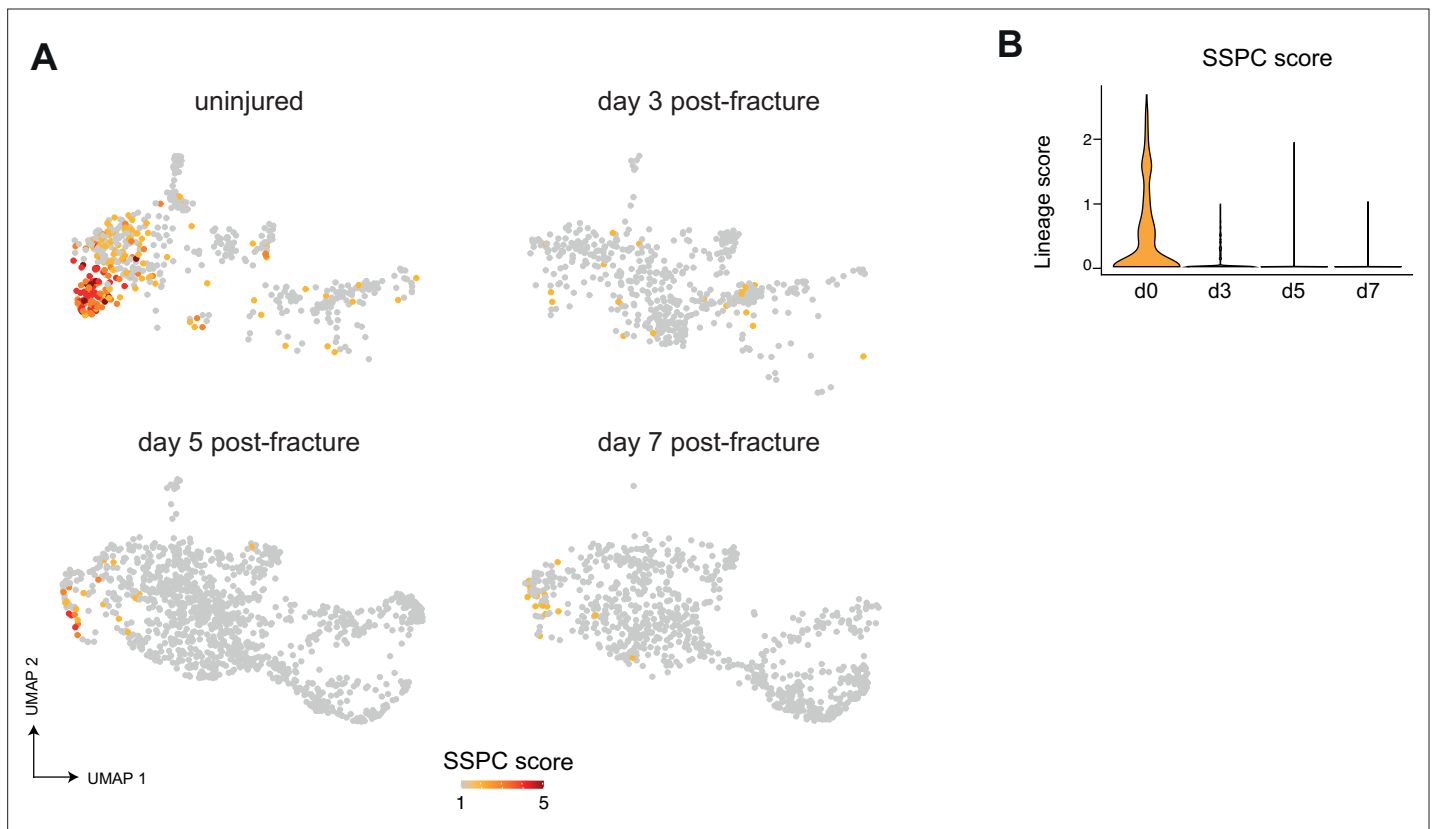


**Figure 4—figure supplement 2.** Absence of skeletal stem/progenitor cells in the injured periosteum. **(A)** Feature plot of SSPC lineage score in the subset of SSPCs, injury-induced fibrogenic cells (IIFCs), osteoblasts, and chondrocytes separated by time point from **Figure 5B**. **(B)** Violin plot of SSPC lineage score by time point.

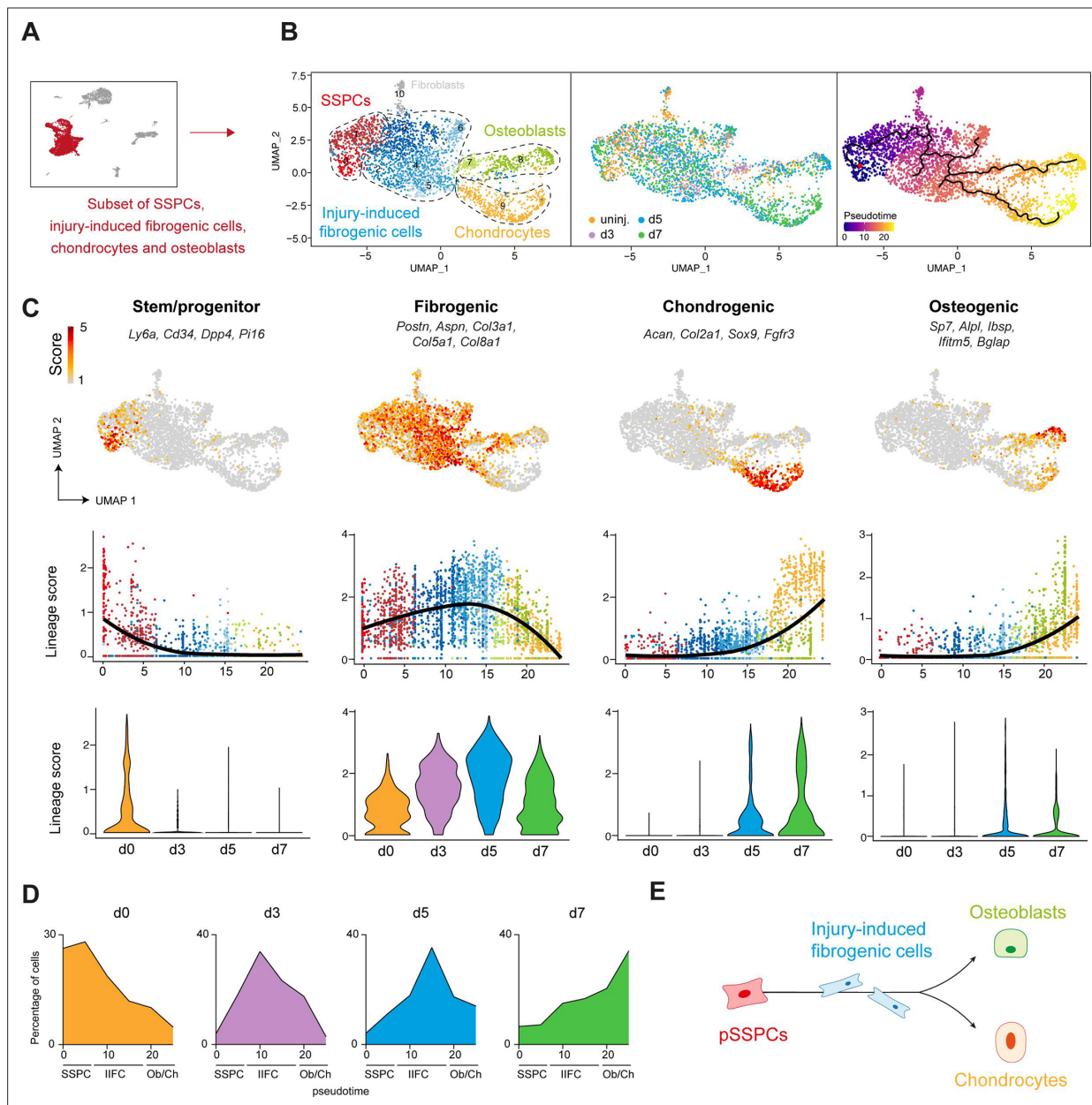


**Figure 5.** Periosteal skeletal stem/progenitor cells activate through a common fibrogenic state prior to undergoing osteogenesis or chondrogenesis. (A) SSPCs, injury-induced fibrogenic cells (IIFCs), chondrocytes, and osteoblasts from integrated uninjured, day 3, 5, and 7 post-fracture samples were extracted for a subset analysis. (B) UMAP of color-coded clustering (left), color-coded sampling (middle), and monoclone pseudotime trajectory (right) of the subset dataset. The four populations are delimited by black dashed lines. (C) (Top) Feature plots of the stem/progenitor, fibrogenic, chondrogenic, and osteogenic lineage scores. (Middle) Scatter plot of the lineage scores along pseudotime. (Bottom) Violin plot of the lineage scores per time point. (D) Distribution of the cells along the pseudotime per time point. (E) Schematic representation of the differentiation trajectories of pSSPCs after fracture.

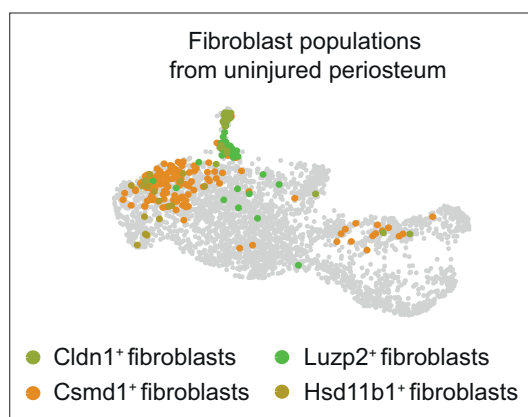


**Figure 5—figure supplement 1.** UMAP highlighting the distribution of periosteal fibroblasts in the combined fracture dataset.

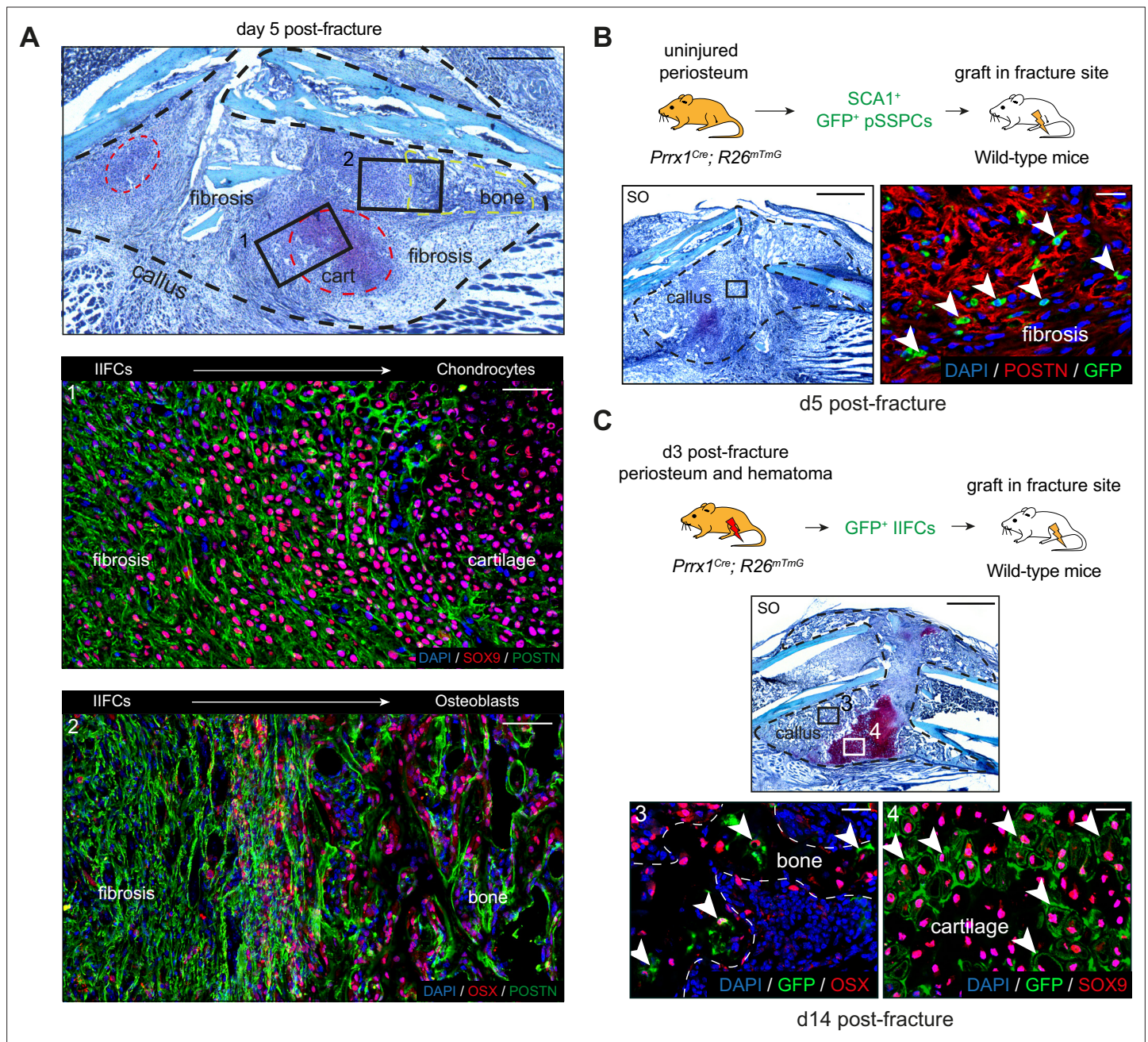


**Figure 6.** In vivo validation of periosteal skeletal stem/progenitor cell differentiation trajectories. **(A)** (Top) Representative Safranin'O staining on longitudinal sections of the hematoma/callus at day 5 post-fracture. The callus is composed of fibrosis, cartilage (red dashed line), and bone (green dashed line). (Middle, box 1) Immunofluorescence on adjacent section shows decreased expression of POSTN (green) and increased expression of SOX9 (red) in the fibrosis-to-cartilage transition zone. (Bottom, box 2) Immunofluorescence on adjacent section shows decreased expression of POSTN (green) and increased expression of OSX (red) in the fibrosis-to-bone transition zone ( $n = 3$  per group). **(B)** Experimental design:  $\text{GFP}^+ \text{SCA1}^+ \text{SSPCs}$  were isolated from uninjured tibia of  $\text{Prrx1}^{\text{Cre}}; \text{R26}^{\text{mTmG}}$  mice and grafted at the fracture site of wild-type mice. Safranin'O staining of callus sections at day 5 post-fracture and high magnification of POSTN immunofluorescence of adjacent section showing that grafted  $\text{GFP}^+ \text{SSPCs}$  contribute to the callus and differentiate into  $\text{POSTN}^+$  IIFCs (white arrowheads) ( $n = 4$  per group). **(C)** Experimental design:  $\text{GFP}^+ \text{IIFCs}$  from periosteum and hematoma at day 3 post-fracture tibia were isolated from  $\text{Prrx1}^{\text{Cre}}; \text{R26}^{\text{mTmG}}$  mice and grafted at the fracture site of wild-type mice. Safranin'O of callus sections at day 14 post-fracture and high magnification of OSX and SOX9 immunofluorescence of adjacent sections showing that grafted  $\text{GFP}^+$  injury-induced fibrogenic cells (IIFCs) contribute to the callus and differentiate into  $\text{OSX}^+$  osteoblasts (box 3, white arrowheads) and  $\text{SOX9}^+$  chondrocytes (box 4, white arrowheads) ( $n = 4$  per group). Scale bars: low magnification: **(A)** 500  $\mu\text{m}$ ; **(B, C)** 1 mm. High magnification: 100  $\mu\text{m}$ .



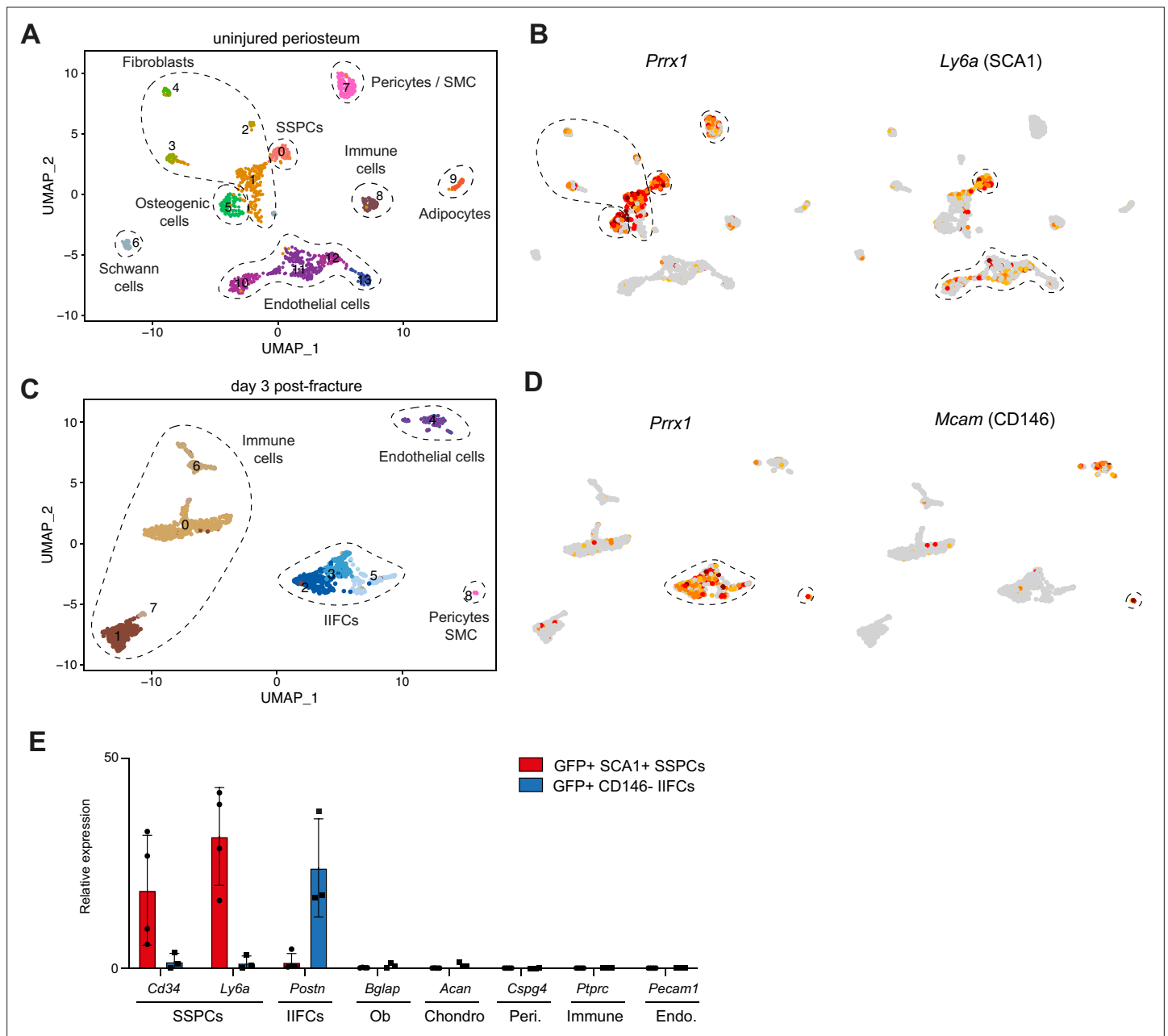


**Figure 6—figure supplement 1.** Validation of skeletal stem/progenitor cell (SSPC) and injury-induced fibrogenic cell (IIFC) sorting strategies. **(A)** UMAP of the clustering of the uninjured periosteum. **(B)** Feature plots of *Prrx1* and *Ly6a* expression in the uninjured dataset. **(C)** UMAP of the clustering of the day 3 post-fracture periosteum and hematoma. **(D)** Feature plots of *Prrx1* and *Mcam* (CD146) expression in the day 3 post-fracture periosteum and hematoma dataset. **(E)** Relative expression of cell population markers by GFP+ SCA1+ SSPCs from uninjured periosteum (n = 4) and GFP+ CD146- IIFCs from day 3 post-fracture periosteum and hematoma (n = 3).

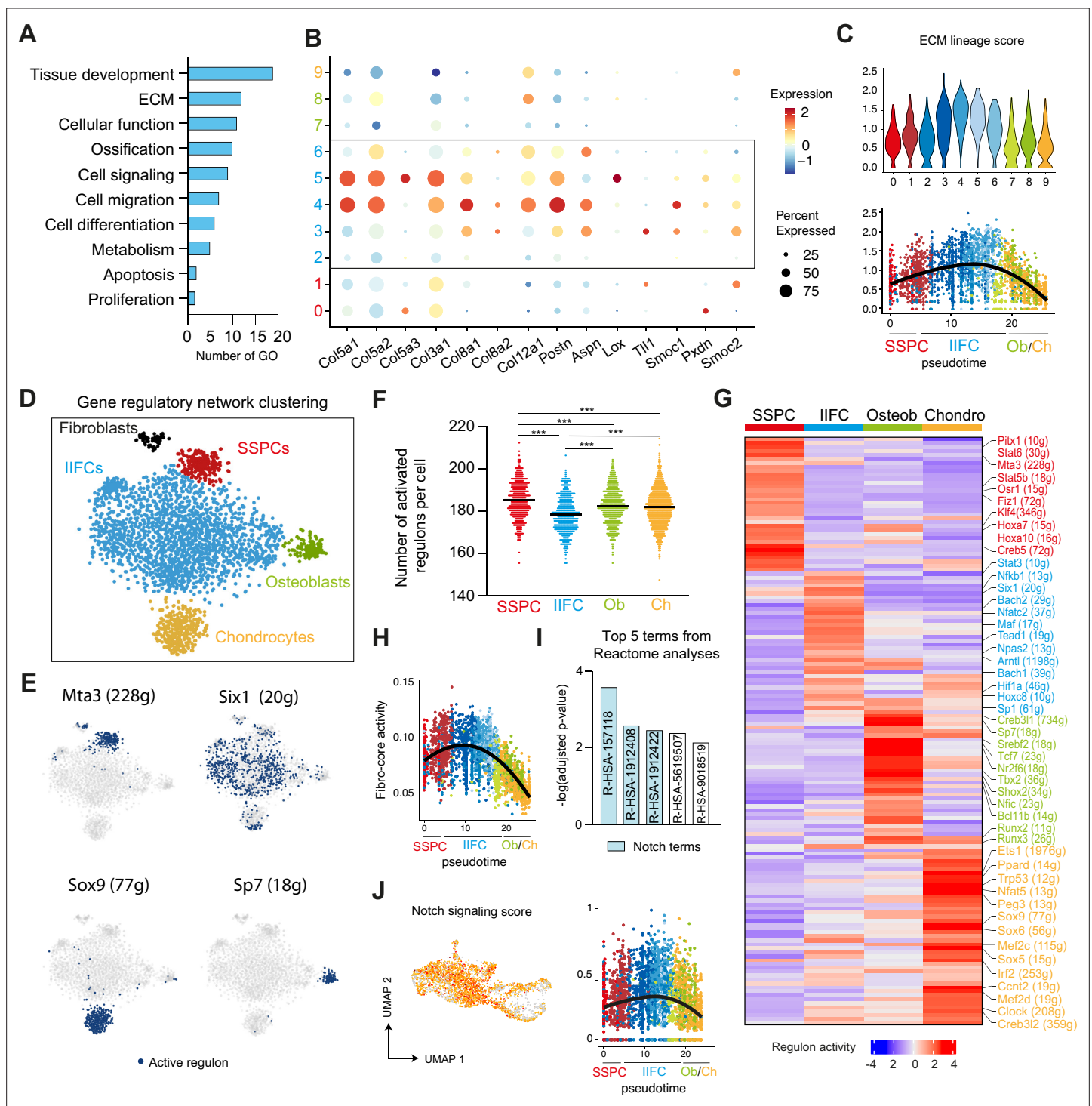


**Figure 7.** Characterization of injury-induced fibrogenic cells. **(A)** Gene Ontology analyses of upregulated genes in injury-induced fibrogenic cells (IIFCs) (clusters 2–6 of UMAP clustering from **Figure 5**). **(B)** Dot plot of extracellular matrix (ECM) genes in UMAP clustering from **Figure 5**. **(C)** Feature plot per cluster and scatter plot along pseudotime of the mean expression of ECM genes. **(D)** Gene regulatory network (GRN)-based tSNE clustering of the subset of skeletal stem/progenitor cells (SSPCs), IIFCs, chondrocytes, and osteoblasts. **(E)** Activation of Mta3, Six1, Sox9, and Sp7 regulons in SSPCs, IIFCs, chondrocytes, and osteoblasts. Blue dots mark cells with active regulon. **(F)** Number of regulons activated per cell in the SSPC, IIFC, osteoblast (Ob), and chondrocyte (Ch) populations. Statistical differences were calculated using one-way ANOVA. \*\*\*p-value < 0.001. **(G)** Heatmap of activated regulons in SSPC, IIFC, osteoblast (osteob), and chondrocyte (chondro) populations. **(H)** Scatter plot of the activity of the combined fibrogenic regulons along monocluster pseudotime from **Figure 5**. **(I)** Reactome pathway analyses of the fibrogenic regulons shows that the three most significant terms are related to Notch signaling (blue). **(J)** Feature plot in Seurat clustering and scatter plot along monocluster pseudotime of the Notch signaling score.

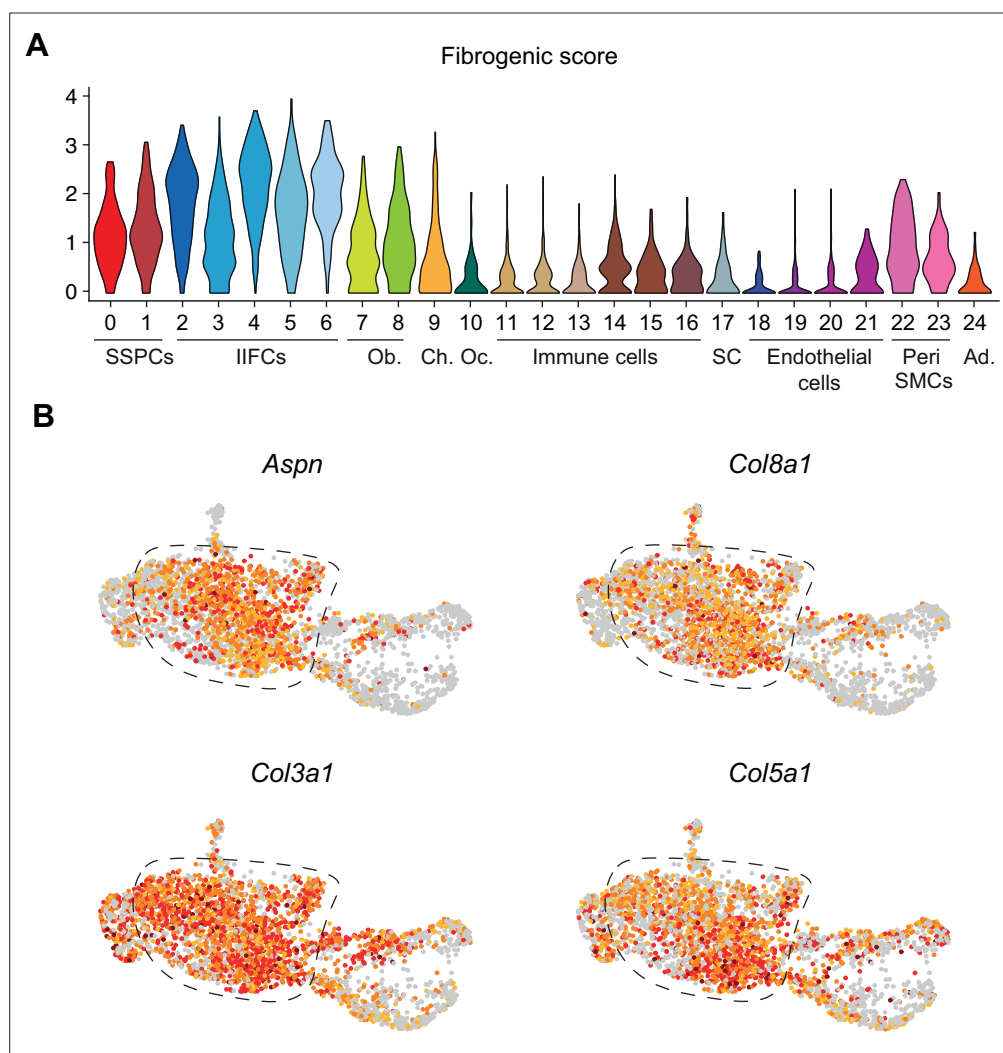


**Figure 7—figure supplement 1.** Injury-induced fibrogenic cells (IIFCs) are expressing extracellular matrix (ECM)-related genes. **(A)** Violin plot of the fibrogenic score in the integrated dataset. **(B)** Feature plots of *Aspn*, *Col3a1*, *Col5a1*, and *Col8a1* in the subset of skeletal stem/progenitor cells (SSPCs), IIFCs, osteoblasts, and chondrocytes.

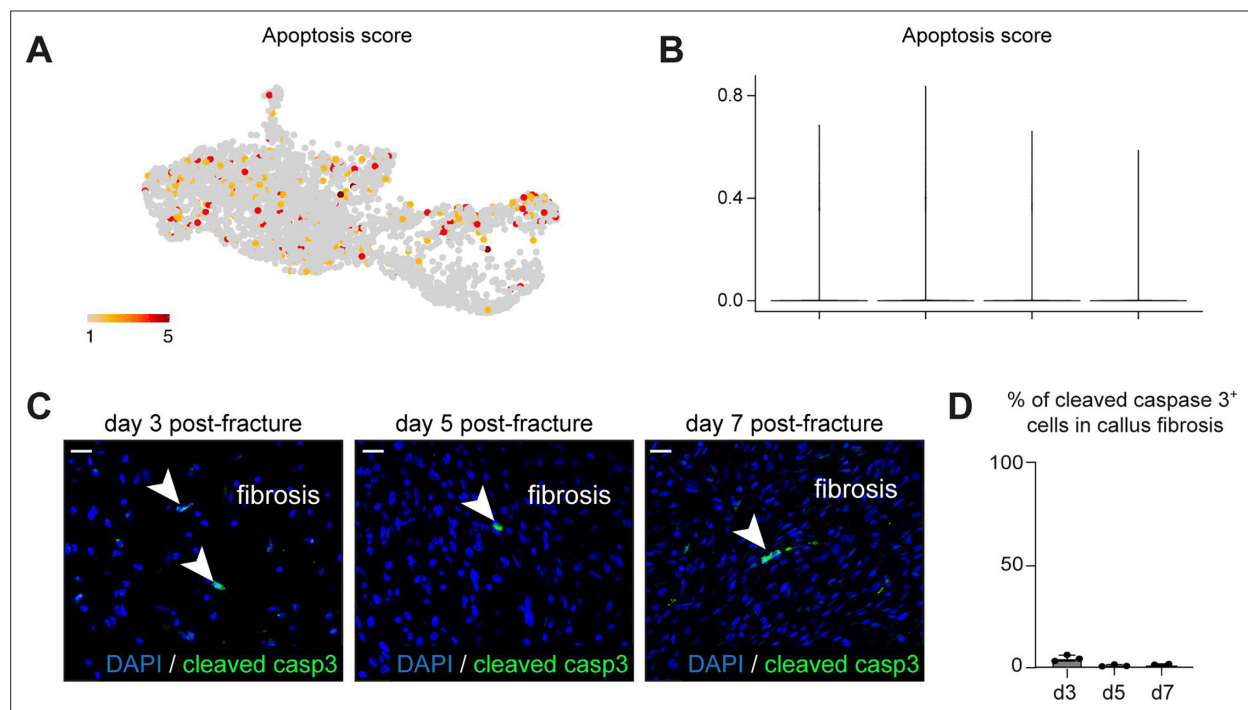


**Figure 7—figure supplement 2.** Injury-induced fibrogenic cells (IIFCs) do not undergo apoptosis. **(A)** Feature plot of the apoptosis score in the subset of skeletal stem/progenitor cells (SSPCs), IIFCs, osteoblast, and chondrocytes. **(B)** Violin plot of the apoptosis score separated by time points. **(C)** Immunofluorescence of cleaved caspase 3 in callus fibrosis at days 3, 5, and 7 post-fracture. **(D)** Percentage of cleaved caspase 3 positive cells in the fibrosis callus fibrosis at day 3 (n = 3), day 5 (n = 3), and day 7 post-fracture (n = 2).



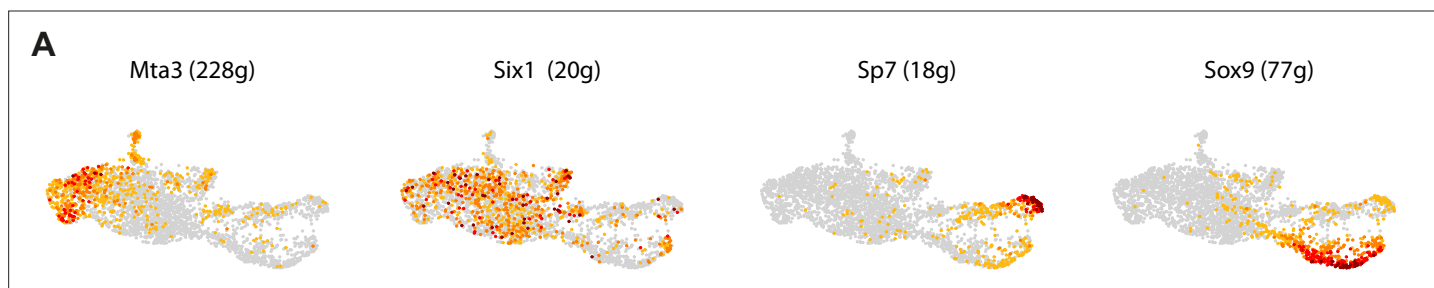


**Figure 7—figure supplement 3.** Activity of lineage specific regulons (Mta3, Six1, Sox9 and Sp7) in the UMAP Seurat clustering of SSPCs, IIFCs, chondrocytes and osteoblasts.

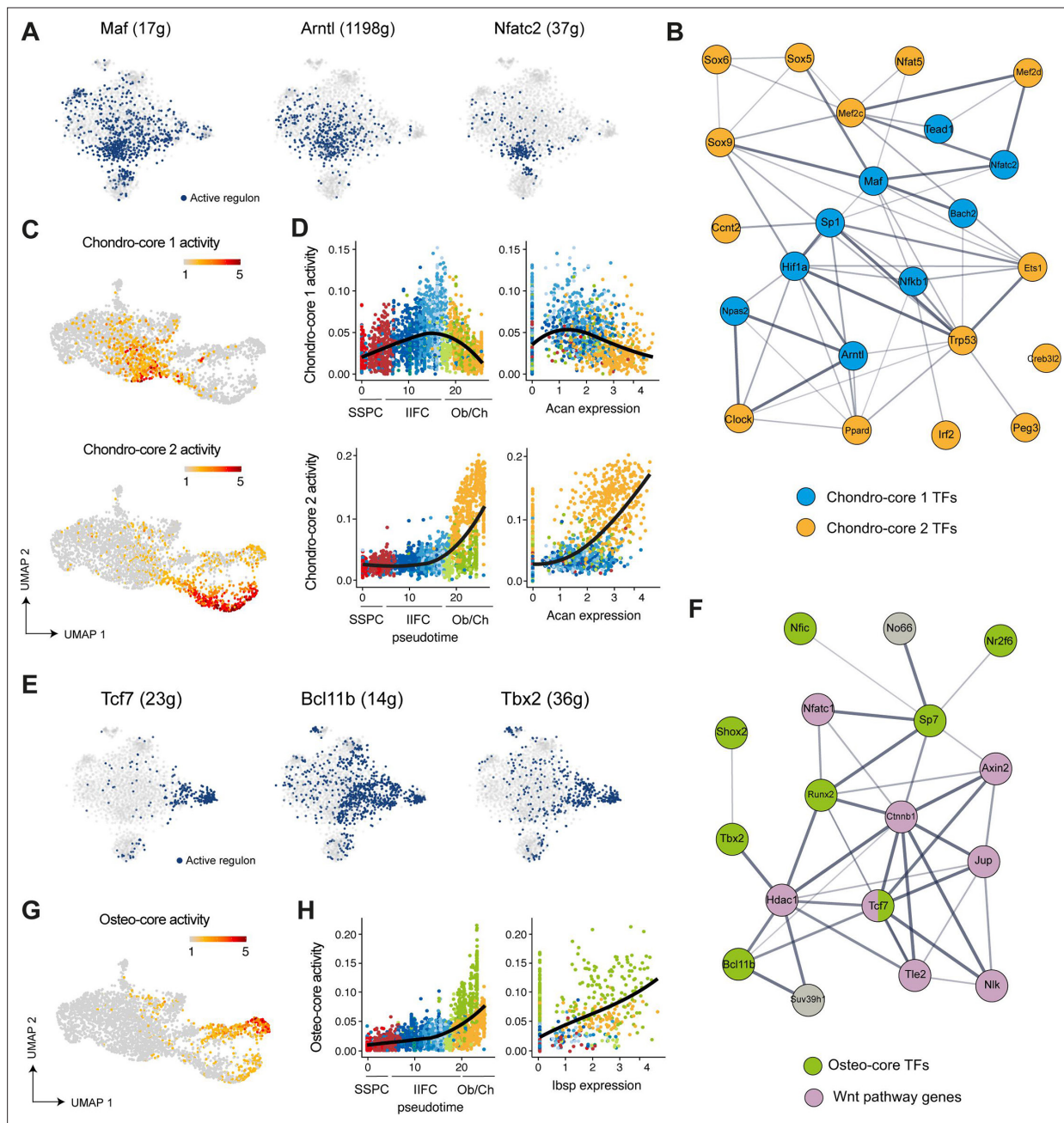


**Figure 8.** Gene regulatory network analyses identify gene cores driving fibrogenic to chondrogenic and osteogenic transitions. **(A)** Activation of Maf, Arntl, and Nfatc2 regulons in skeletal stem/progenitor cells (SSPCs), injury-induced fibrogenic cells (IIFCs), chondrocytes, and osteoblasts. **(B)** STRING interaction network of the chondro-core 1 and 2 transcription factors (blue and orange, respectively). **(C)** Feature plot of chondro-core 1 (top) and chondro-core 2 (bottom) activities in SSPCs, IIFCs, chondrocytes, and osteoblasts in Seurat UMAP from **Figure 5**. **(D)** Scatter plot of chondro-core 1 (top) and chondro-core 2 (bottom) activities along monoclone pseudotime and Acan expression. **(E)** Activation of Tcf7, Bcl11b, and Tbx2 regulons in SSPCs, IIFCs, chondrocytes, and osteoblasts. **(F)** STRING interaction network of the osteo-core transcription factors (green) and their related genes shows that most of osteo-core related genes are involved in Wnt pathway (purple). **(G)** Feature plot of the osteo-core activity in SSPCs, IIFCs, chondrocytes, and osteoblasts in Seurat UMAP from **Figure 5**. **(H)** Scatter plot of osteo-core activity along monoclone pseudotime and Ibsp expression.

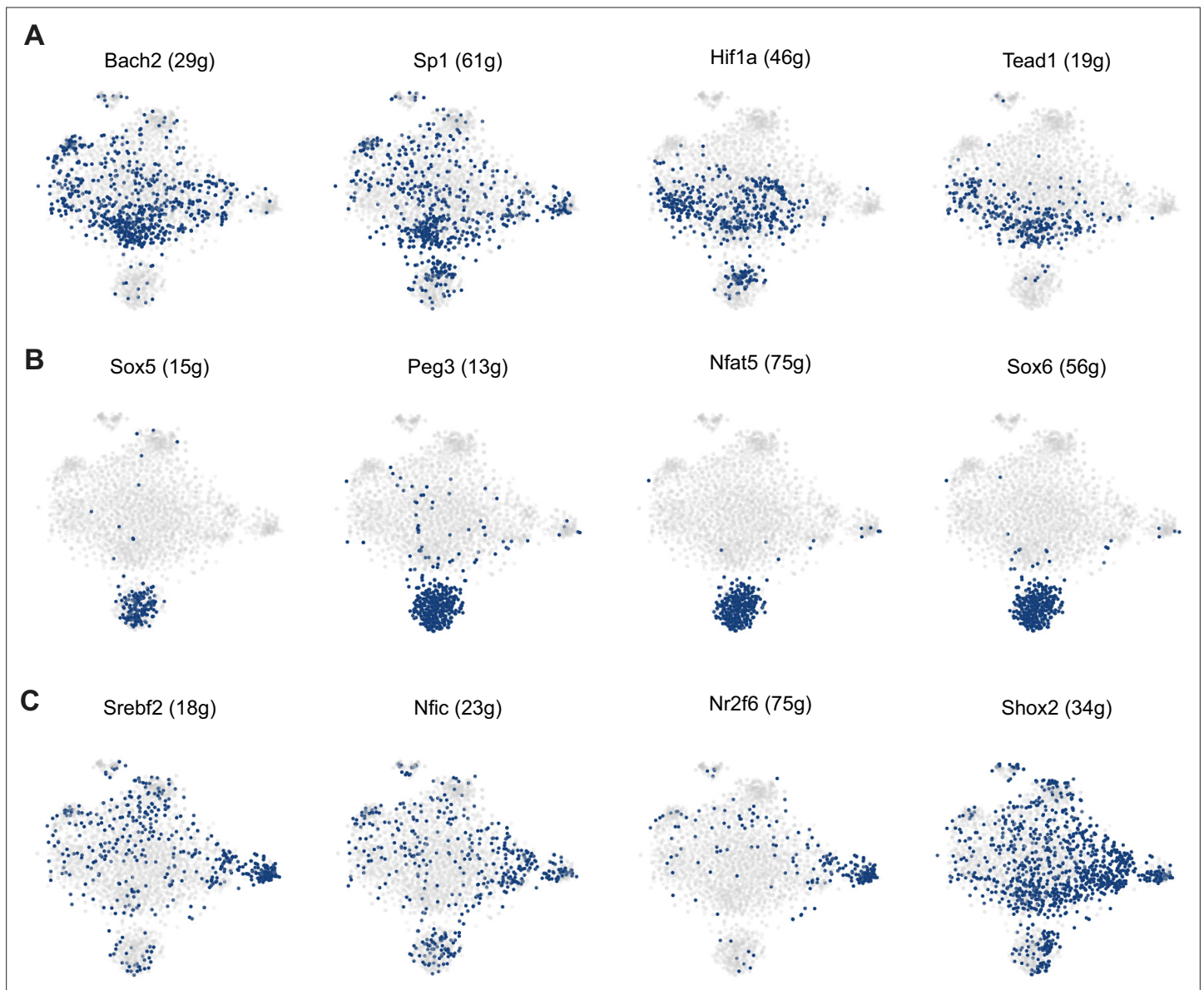


**Figure 8—figure supplement 1.** Regulon activity in the subset of skeletal stem/progenitor cells (SSPCs), injury-induced fibrogenic cells (IIFCs), osteoblasts, and chondrocytes. **(A)** Activity of chondro-core 1 regulons in SCENIC tSNE clustering of SSPCs, IIFCs, chondrocytes, and osteoblasts. **(B)** Activity of chondro-core 2 regulons in SCENIC tSNE clustering of SSPCs, IIFCs, chondrocytes, and osteoblasts. **(C)** Activity of osteo-core regulons in SCENIC tSNE clustering of SSPCs, IIFCs, chondrocytes, and osteoblasts.

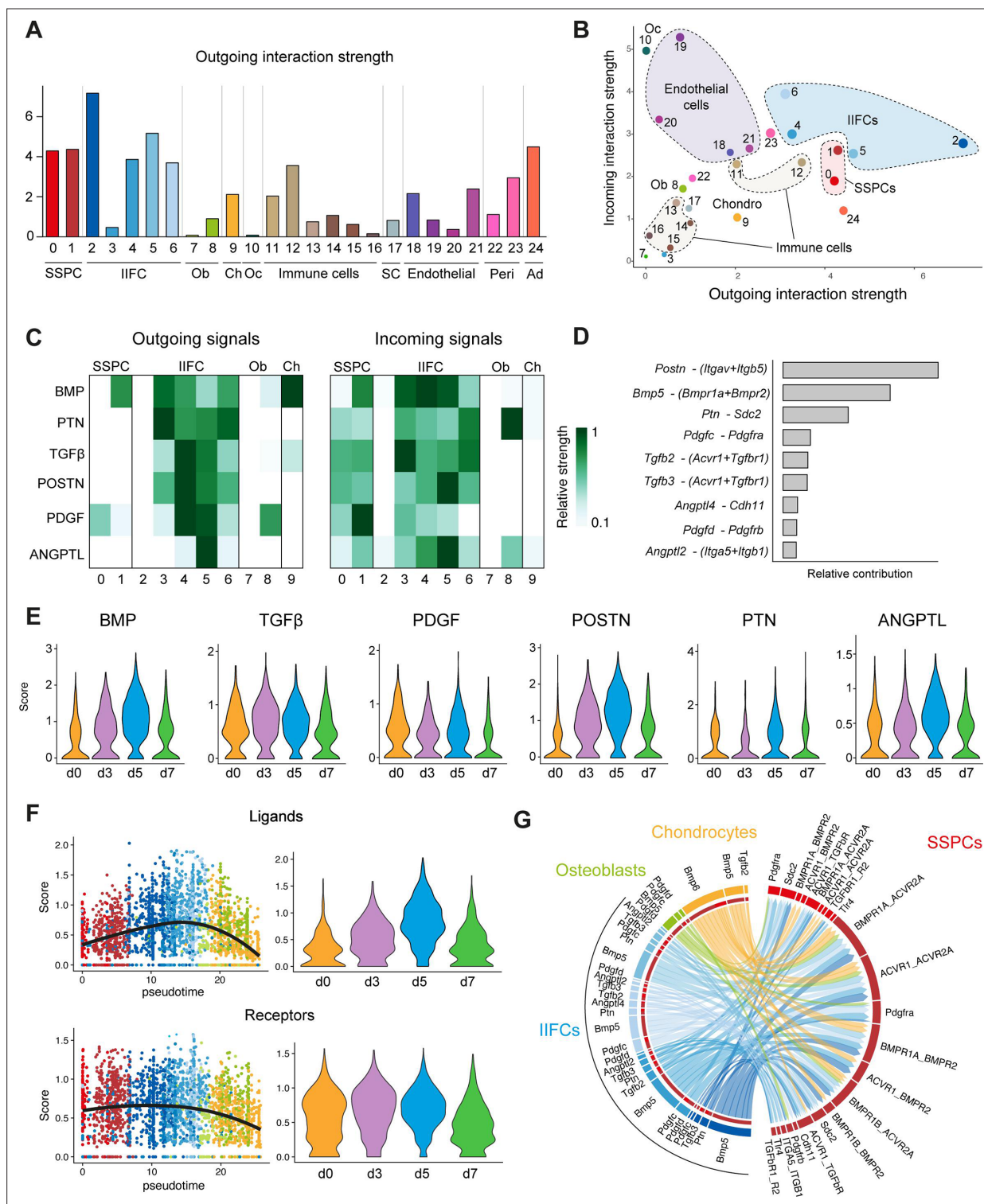


**Figure 9.** Injury-induced fibrogenic cells are the main source of paracrine factors after fracture. **(A)** Outgoing interaction strengths of the different cell populations of the fracture environment determined using CellChat package. **(B)** Comparison of incoming and outgoing interaction strengths across SSPC, IIFC, chondrogenic, and osteogenic populations. **(C)** Outgoing and incoming signaling from and to SSPCs, IIFCs, chondrocytes, and osteoblasts. **(D)** Cell–cell interactions identified between SSPCs, IIFCs, chondrocytes, and osteoblasts. **(E)** Violin plots of the score of BMP, TGFβ, PDGF, POSTN, PTN, and ANGPTL signaling per time point. **(F)** Scatter plot along pseudotime and violin plot per time point of the mean expression of the ligand and receptors involved in signaling from IIFCs. **(G)** Circle plot of the interactions between SSPCs, IIFCs, chondrocytes, and osteoblasts, showing that most signals received by SSPCs are coming for IIFCs. Ob: osteoblasts; Oc: osteoclasts; Ch: chondrocytes; SC: Schwann cells; Ad: adipocytes.

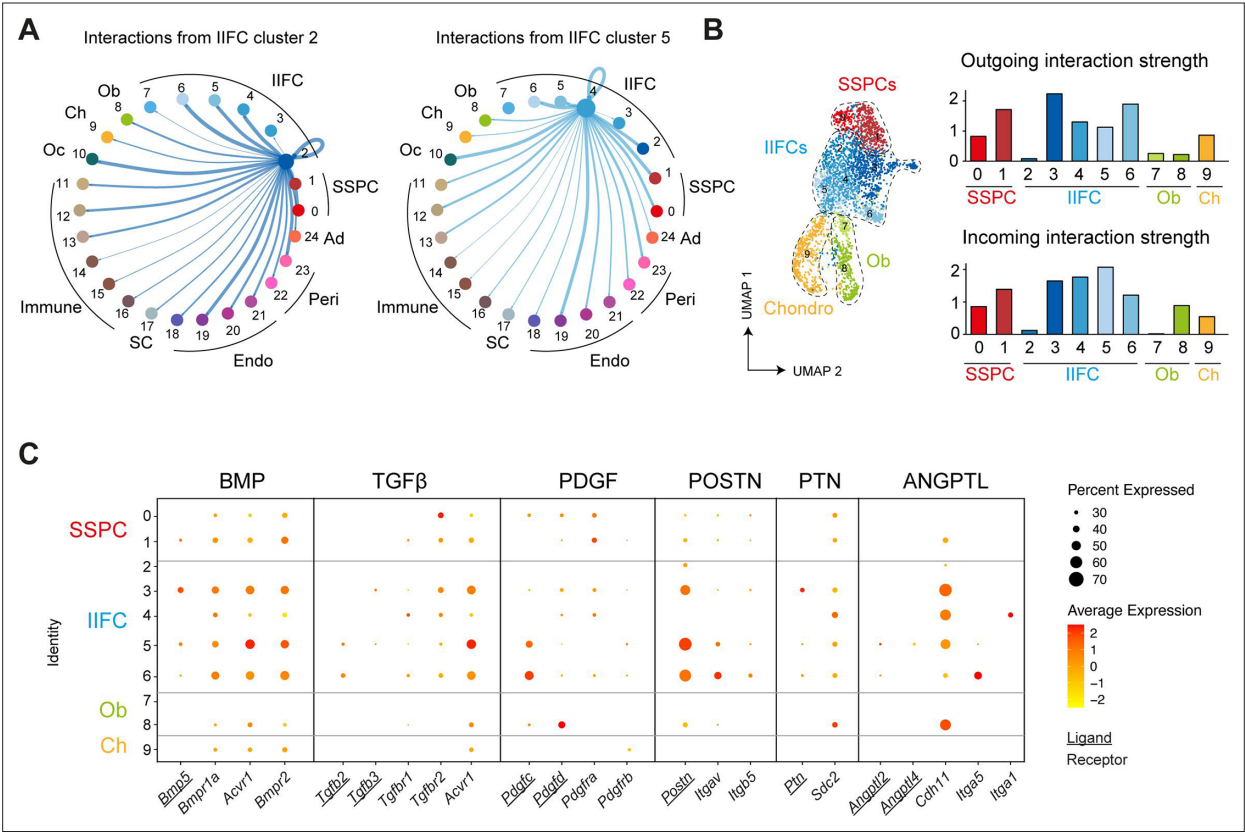


**Figure 9—figure supplement 1.** Paracrine interactions from injury-induced fibrogenic cells (IIFCs). **(A)** Circle plots showing the interaction strengths between IIFCs in clusters 2 and 5 with the other cell populations. **(B)** (Left) Feature plot of the subset of SSPCs, IIFCs, chondrocytes and osteoblasts from **Figure 5**. (Right) Outgoing and incoming interaction strengths of the subset of skeletal stem/progenitor cells (SSPCs), IIFCs, chondrocytes, and osteoblasts. **(C)** Dot plots of the expression of the ligands (underlined) and receptors of BMP, TGFβ, PDGF, POSTN, PTN, and ANGPTL family involved in cell–cell interactions from IIFCs after fracture.



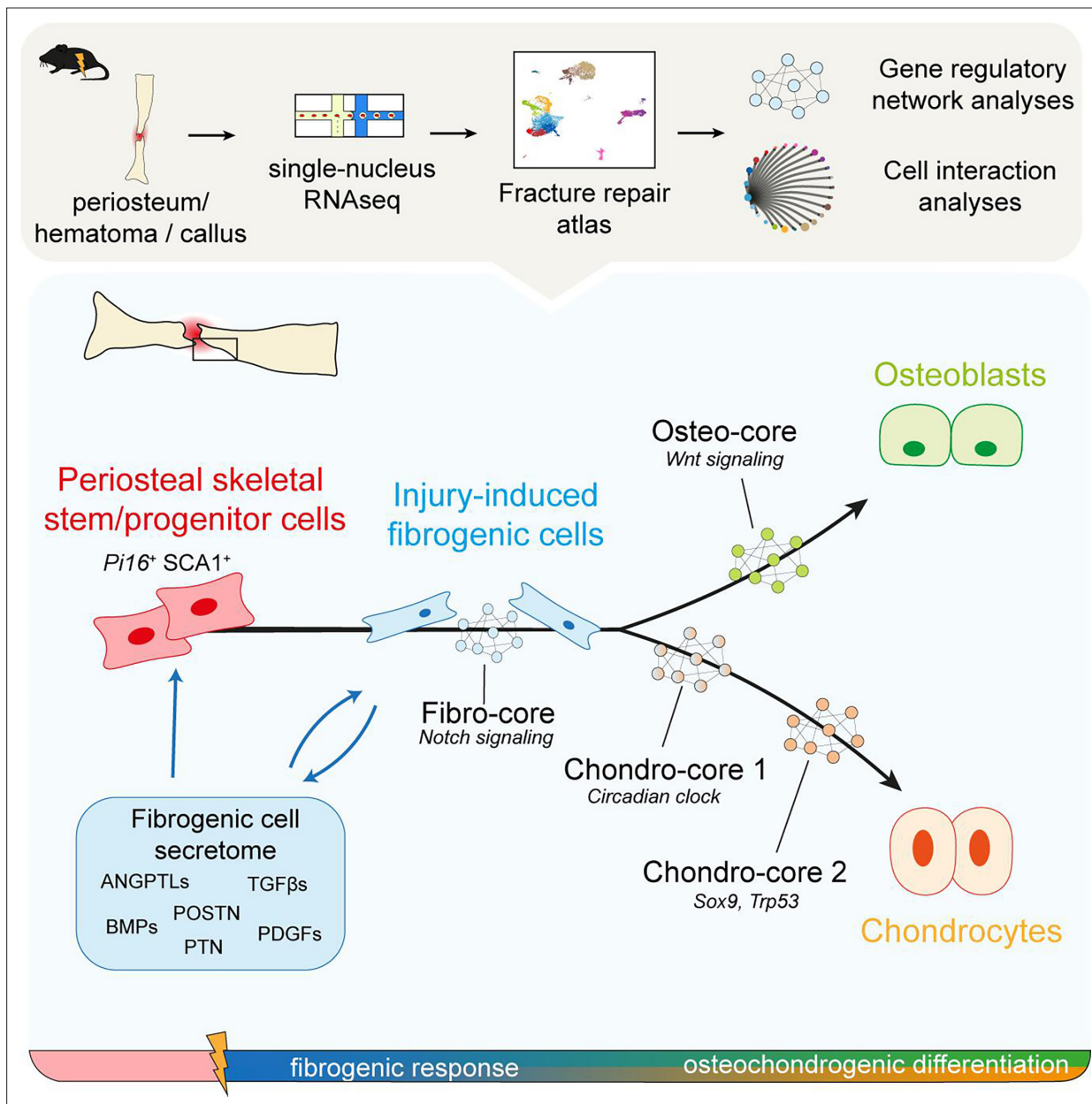


**Figure 10.** Activation and differentiation trajectories of periosteal skeletal stem/progenitor cells (SSPCs) after fracture.